nature medicine

Activation of PKC-δ and SHP-1 by hyperglycemia causes vascular cell apoptosis and diabetic retinopathy

Pedro Geraldes[1], Junko Hiraoka-Yamamoto[1], Motonobu Matsumoto[1], Allen Clermont[1], Michael Leitges[3], Andre Marette[4], Lloyd P Aiello[1,2,5], Timothy S Kern[6] & George L King[1,7]

Cellular apoptosis induced by hyperglycemia occurs in many vascular cells and is crucial for the initiation of diabetic pathologies. In the retina, pericyte apoptosis and the formation of acellular capillaries, the most specific vascular pathologies attributed to hyperglycemia, is linked to the loss of platelet-derived growth factor (PDGF)-mediated survival actions owing to unknown mechanisms. Here we show that hyperglycemia persistently activates protein kinase C-δ (PKC-δ, encoded by *Prkcd*) and p38α mitogen-activated protein kinase (MAPK) to increase the expression of a previously unknown target of PKC-δ signaling, Src homology-2 domain–containing phosphatase-1 (SHP-1), a protein tyrosine phosphatase. This signaling cascade leads to PDGF receptor-β dephosphorylation and a reduction in downstream signaling from this receptor, resulting in pericyte apoptosis independently of nuclear factor-κB (NF-κB) signaling. We observed increased PKC-δ activity and an increase in the number of acellular capillaries in diabetic mouse retinas, which were not reversible with insulin treatment that achieved normoglycemia. Unlike diabetic age-matched wild-type mice, diabetic *Prkcd*$^{-/-}$ mice did not show activation of p38α MAPK or SHP-1, inhibition of PDGF signaling in vascular cells or the presence of acellular capillaries. We also observed PKC-δ, p38α MAPK and SHP-1 activation in brain pericytes and in the renal cortex of diabetic mice. These findings elucidate a new signaling pathway by which hyperglycemia can induce PDGF resistance and increase vascular cell apoptosis to cause diabetic vascular complications.

A common cellular pathology for many diabetic vascular complications is an enhanced rate of cellular apoptosis as observed in retinal pericytes, renal podocytes and vascular endothelial cells[1,2]. Hyperglycemia, the major risk factor for diabetic microvascular complications[3], is responsible for inducing apoptosis in these vascular tissues directly[4] or indirectly[5,6] by altering cytokine expression and leading to the accumulation of toxic products in organs affected by diabetes. Although intensive insulin treatment in individuals with diabetes can delay the onset and progression of diabetic complications[3], initiation of intensive glycemic control after periods of poor glycemia does not substantially decrease the rate of progression of retinopathy and other microvascular diseases, suggesting that hyperglycemia-induced chronic cellular changes are difficult to reverse[7]. To clarify the biochemical mechanisms involved in hyperglycemia-induced cellular apoptosis, we characterized the signaling cascade of hyperglycemia leading to pericyte apoptosis in diabetic retinopathy, the most specific vascular pathology attributed to diabetes, which may represent a common pathway for other microvascular abnormalities in diabetes[8,9].

Noteworthy recent findings implicate a role of PDGF receptor-β (PDGFR-β) in pericyte apoptosis. PDGF-B or PDGFR-β deficient mice show retinal pericyte depletion associated with the development of microaneurysms and acellular capillaries as a result of both pericyte and endothelial cell death, recapitulating the early changes of diabetic retinopathy[10]. However, it is unclear whether pericyte loss results from decreased PDGF-B abundance, as the expression of PDGF-B in the retina is increased in diabetic compared to nondiabetic rats[11]. In addition, although oxidative stress and activation of NF-κB have been reported to be involved in hyperglycemia-induced cell apoptosis, the interrelationship between PDGF-B inhibition and oxidative stress in mediating pericyte apoptosis and the initiation of diabetic retinopathy is not known. In investigating the mechanisms by which hyperglycemia induces pericyte apoptosis, we have uncovered a new signaling pathway by which hyperglycemia induces vascular damage: activation of PKC-δ and p38α MAPK, leading to increased expression of the protein tyrosine phosphatase (PTP) SHP-1, which, in turn, leads to the dephosphorylation of PDGFR-β.

RESULTS

PKC-δ affects PDGF resistance and acellular capillary formation

As PKC activation is associated with retinal and vascular pathologies of diabetes[12], we studied the effects of PKC activation on PDGF signaling inhibition and pericyte apoptosis. *In situ* PKC activity increased by 40% (P = 0.028) in mouse retina after 3 months of diabetes (**Fig. 1a**). Immunoblot analyses showed that the amounts of both the PKC-β2 and PKC-δ isoforms were increased (P = 0.022 and P = 0.043,

[1]Dianne Nunnally Hoppes Laboratory for Diabetes Complications and [2]Beetham Eye Institute of Joslin Diabetes Center, Boston, Massachusetts, USA. [3]The Biotechnology Centre of Oslo, University of Oslo, Oslo, Norway. [4]Department of Anatomy and Physiology, Université Laval, Québec, Québec, Canada. [5]Department of Ophthalmology, Harvard Medical School, Boston, Massachusetts, USA. [6]Department of Medicine, Case Western Reserve University, Cleveland, Ohio, USA. [7]Department of Medicine, Harvard Medical School, Boston, Massachusetts, USA. Correspondence should be addressed to G.L.K. (george.king@joslin.harvard.edu).

Received 25 March; accepted 22 September; published online 1 November 2009; doi:10.1038/nm.2052

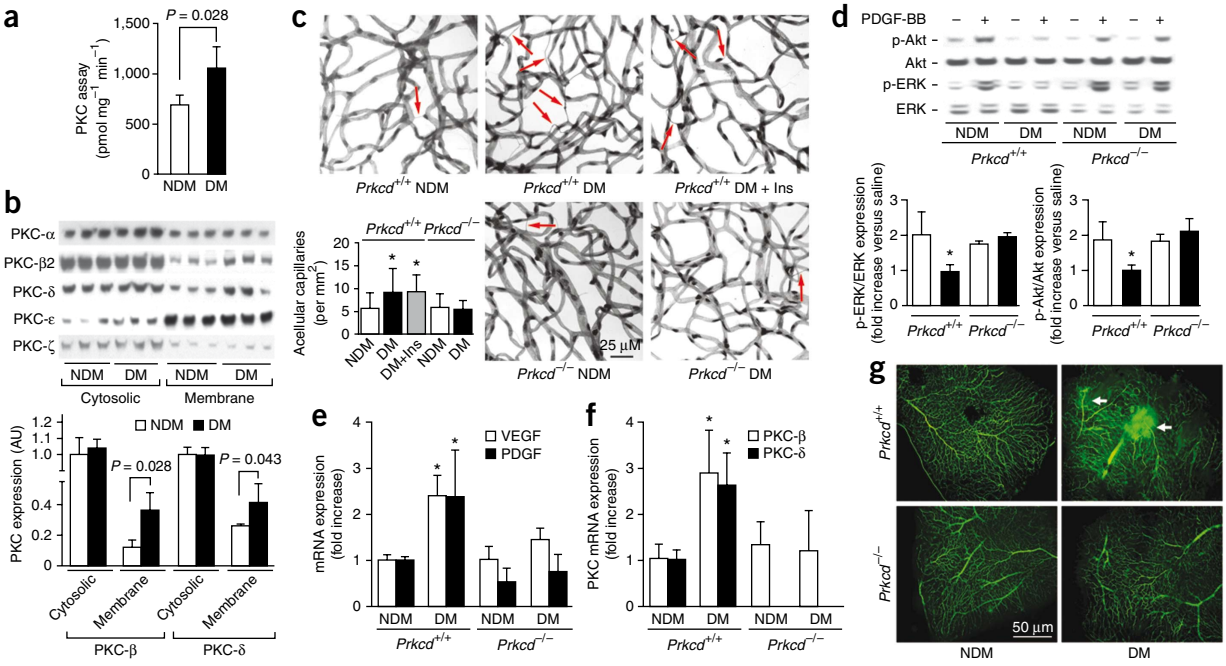

Figure 1 PKC-δ activation causes PDGF-B inhibition and the formation of acellular capillaries. (**a**) *In situ* PKC activity assay, as measured in retinas of mice diabetic for 3 months (DM mice, $n = 6$) as compared to nondiabetic mice (NDM mice, $n = 6$). (**b**) Immunoblot analyses of PKC isoforms in the cytosolic and membrane fractions of retinal isolated microvessels of NDM and DM mice (top) and densitometric quantification (bottom) ($n = 4$). (**c**) Hematoxylin and periodic acid-Schiff staining of retinal vasculature indicating acellular capillaries (red arrows). Bottom left, quantification of acellular capillaries in *Prkcd*$^{+/+}$ and *Prkcd*$^{-/-}$ mouse retinas (NDM *Prkcd*$^{+/+}$, $n = 22$; DM *Prkcd*$^{+/+}$, $n = 19$; DM + insulin (Ins) *Prkcd*$^{+/+}$, $n = 12$; NDM *Prkcd*$^{-/-}$, $n = 13$; DM *Prkcd*$^{-/-}$, $n = 13$). (**d**) Immunoblot analyses of Atk and ERK phosphorylation after intravitreous injection of saline or PDGF-BB into NDM and DM mouse retinas (top) and densitometric quantification (bottom) ($n = 3$). (**e**,**f**) Expression of VEGF and PDGF (**e**) and PKC-β and PKC-δ (**f**) mRNA in isolated microvessels from NDM and DM *Prkcd*$^{+/+}$ or *Prkcd*$^{-/-}$ mice ($n = 6$). (**g**,**h**) Flat mounts of retinas infused with FITC-dextran (**g**) and permeability assay using Evans blue dye ($n = 8$) (**h**). Results are shown as means ± s.d. of three or four independent experiments. *$P < 0.05$ versus NDM *Prkcd*$^{+/+}$ mice.

respectively) in membrane fractions of isolated retinal microvessels (**Fig. 1b**) and whole retina (**Supplementary Fig. 1a**). PKC-δ activation induces apoptosis in other cell types[13]. Therefore, we evaluated retinal vascular changes in nondiabetic and diabetic PKC-δ–null (*Prkcd*$^{-/-}$) and age-matched control (*Prkcd*$^{+/+}$) mice with or without interventional glycemic control with insulin implants. Six months after the streptozotocin treatment used to induce diabetes, *Prkcd*$^{+/+}$ and *Prkcd*$^{-/-}$ diabetic mice had lower body weights and plasma insulin levels but increased glucose concentrations compared with nondiabetic mice with a similar genetic background (**Supplementary Fig. 1b**). Treatment of the diabetic mice using insulin implants for the last 3 months of the experiment normalized their body weight and glucose level but not their hyperinsulinemia (**Supplementary Table 1**). Histological analyses of the retina showed that diabetes increased the number of acellular capillaries by 59% ($P < 0.05$) (**Fig. 1c**) and the combined numbers of acellular capillaries and pericyte loss (ghosts) (**Supplementary Fig. 1c**,**d**) in *Prkcd*$^{+/+}$ but not *Prkcd*$^{-/-}$ mice as compared to nondiabetic *Prkcd*$^{+/+}$ mice. Reduction in blood glucose levels for the last 3 months of the experiment did not prevent the increase in the number of acellular capillaries in *Prkcd*$^{+/+}$ mice (**Fig. 1c**).

Endothelial-specific PDGF-B–deficient mice show pericyte loss, microaneurysm formation and acellular capillaries in the retina[10]. In view of our findings that PKC-δ activation also leads to these types of retinal vascular defects, we evaluated whether the ability of PDGF-B to activate the protein kinases extracellular signal–related kinase (ERK) and Akt in the retina is affected by PKC. After intravitreous injection of PDGF-BB (dimeric PDGF composed of two B chains), the levels of phospho-ERK and phospho-Akt in the retina of nondiabetic *Prkcd*$^{+/+}$ mice and nondiabetic and diabetic *Prkcd*$^{-/-}$ mice increased by 1.6- to 2.1-fold ($P < 0.05$) but remained unchanged in diabetic *Prkcd*$^{+/+}$ mice (**Fig. 1d**). Vascular endothelial growth factor (VEGF), PDGF-B, PKC-β and PKC-δ mRNA or protein expression increased in isolated retinal microvessels (**Fig. 1e**,**f**) and in whole retina (**Supplementary Fig. 2a–c**) of diabetic as compared with nondiabetic *Prkcd*$^{+/+}$ mice by 2.4- to 2.9-fold ($0.001 < P < 0.05$). Normalization of blood glucose concentrations did not prevent the increases in PDGF-B or PKC-δ protein or mRNA expression induced by diabetes (**Supplementary Fig. 2a–c**). Consistent with the histological retinal findings, PDGF-B, PKCβ and VEGF protein and mRNA expression were not higher in diabetic *Prkcd*$^{-/-}$ mice as compared to nondiabetic *Prkcd*$^{-/-}$ mice (**Fig. 1e**,**f** and **Supplementary Fig. 2a–c**). Moreover, phosphorylation of PKC-δ (on Tyr311) was higher in diabetic as compared with nondiabetic *Prkcd*$^{+/+}$ mice, confirming activation of the PKC-δ isoform in retinas of diabetic mice (**Supplementary Fig. 2a**). Diabetic *Prkcd*$^{+/+}$ but not *Prkcd*$^{-/-}$ mice showed increased leakage and permeability ($P = 0.038$) compared to nondiabetic *Prkcd*$^{+/+}$, as assessed by flat mounts of retinas injected with FITC-dextran (**Fig. 1g**) and Evans blue (**Fig. 1h**). *Prkcd*$^{+/+}$ mice after 4 weeks of diabetes had a 46% reduction of retinal blood flow (RBF) ($P < 0.05$) and a 78% increase in mean circulation time (MCT) ($P < 0.01$) as compared to nondiabetic *Prkcd*$^{+/+}$ mice (**Supplementary Fig. 3a**,**b**). Notably, diabetic *Prkcd*$^{-/-}$ mice also showed a decrease

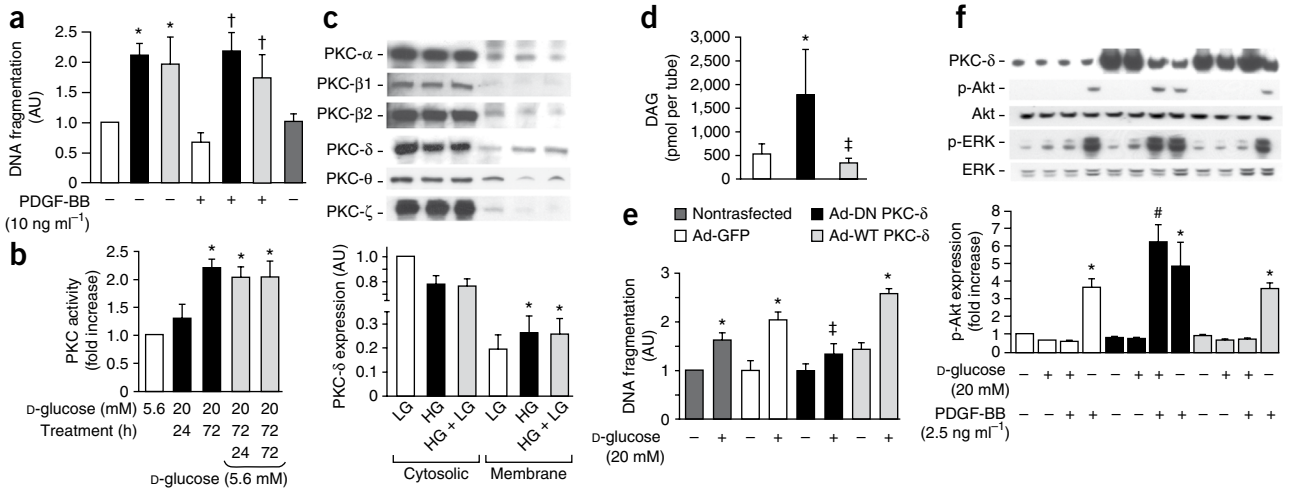

Figure 2 Hyperglycemia inhibits PDGF-B actions and induces pericyte apoptosis through activation of PKC-δ. (**a**) DNA fragmentation in BRPCs incubated with low glucose (5.6 mM, LG, white bars), high glucose (HG, 20 mM) for 72 h without (black bars) or with LG for an additional 72 h (HG + LG, gray bars) in the absence or presence of PDGF-BB. (**b**) *In situ* PKC activity measured in BRPCs exposed to the indicated glucose conditions. (**c**) Immunoblot analyses of PKC isoforms in the cytosolic and membrane fractions of BRPCs exposed to the indicated glucose conditions. (**d**) Total diacylglycerol (DAG) levels (measured as described in the Online Methods) in BRPCs exposed to LG (white bar), HG (black bar) or HG + LG (gray bar). (**e**,**f**) BRPCs were transfected with Ad-GFP, Ad-DN PKC-δ or Ad-WT PKC-δ as indicated and incubated with LG (–) or HG (+) for 72 h. (**e**) DNA fragmentation. (**f**) Immunoblot analyses of PKC-δ, phospho-ERK, ERK, phospho-Akt and Akt (top) and densitometric quantification (bottom) with or without addition of PDGF-BB, as indicated. Results are shown as means ± s.d. of three to five independent experiments. *$P < 0.01$ versus LG, †$P < 0.05$ versus PDGF-BB in LG, ‡$P < 0.05$ versus HG or Ad-GFP transfected cells in HG, #$P < 0.01$ versus HG + PDGF-BB in Ad-GFP–transfected cells.

in RBF and an increase in MCT versus nondiabetic *Prkcd*$^{-/-}$ mice (**Supplementary Fig. 3a**,**b**). The alteration of RBF in mice by hyperglycemia seems to be transient, as blood flow returned to basal levels after a 2-month period of diabetes (**Supplementary Fig. 3c**). Although hyperglycemia-induced endothelin-1 (ET-1) expression in the retina is related to retinal abnormalities[14], transgenic mice overexpressing ET-1 showed decreased RBF (**Supplementary Fig. 3d**) but did not develop vascular pathologies even after 12 months of age (data not shown). These results suggest that early changes of slowed RBF may not predict development of diabetic retinopathy.

Effects of high glucose on PKC-δ and PDGF-B signaling

To identify the mechanisms by which glucose levels and PKC-δ isoform activation may inhibit PDGF-B action and increase pericyte apoptosis, we developed a cultured bovine retinal pericyte (BRPC) model that mimics the chronic effects of hyperglycemia on retinal pericyte pathology (**Supplementary Fig. 4a**). Exposure of BRPCs to a high concentration of glucose (20 mM; 'high glucose') for 72 h increased DNA fragmentation by twofold ($P < 0.01$) and increased annexin V marker abundance by 11.6% as compared to a low concentration of glucose (5.6 mM; 'low glucose') (**Fig. 2a** and **Supplementary Fig. 4b**). Decreasing the glucose concentration from high to low for an additional period of 3 d did not prevent pericyte apoptosis (**Fig. 2a**). Stimulation with PDGF-BB decreased DNA fragmentation by 31% ($P < 0.05$) in the low-glucose condition. However, PDGF-BB did not prevent high glucose–induced DNA fragmentation, even when tested on BRPCs that had been switched to low glucose levels for an additional period of 3 days (**Fig. 2a**). Retinal pericytes isolated from Sprague-Dawley rats that had been rendered diabetic for three months retained an elevated level of apoptosis when cultured either in low-glucose or high-glucose conditions as compared to retinal pericytes isolated from nondiabetic rats (**Supplementary Fig. 4c**). Incubation of BRPCs in high-glucose or in high-glucose followed by low-glucose conditions increased expression of proapoptotic molecules such as cleaved caspase-3 and Bax and decreased the expression of the anti-apoptotic protein Bcl-2 as compared to incubation in low-glucose conditions (**Supplementary Fig. 4d**). PDGF-BB increased DNA synthesis by 2.5-fold ($P < 0.01$) in BRPCs at low glucose concentrations; this effect was inhibited by 100% when pericytes were exposed to high-glucose and PDGF-B conditions for 3 d (**Supplementary Fig. 4e**). *In situ* total PKC activity and PKC-δ activity in BRPCs increased by 100% and 30%, respectively ($P < 0.05$), in a time-dependent manner after 72 h of exposure to high glucose and remained elevated after the cells were switched to low-glucose conditions (**Fig. 2b** and **Supplementary Fig. 5a**). Immunoblot analyses showed that PKC-δ was translocated from the cytosol to the membrane fraction when pericytes were incubated with high glucose (39%, $P < 0.05$) and remained in the membrane fraction even when the cells were returned to low glucose conditions (**Fig. 2c**).

The total amount of diacylglycerol, an activator of PKCs, increased by 2.3-fold ($P < 0.05$) in BRPCs exposed to high-glucose conditions for 72 h (**Fig. 2d**). In contrast to PKC activation, switching BRPCs from high- to low-glucose conditions did reverse the increase in diacylglycerol levels (**Fig. 2d**). Although the half-life of PKC-δ mRNA, as determined in experiments using actinomycin D, was not affected by high glucose compared to low glucose, PKC-δ mRNA levels increased by 2.7-fold ($P < 0.05$) when pericytes were exposed to high glucose, an effect that was not reversed by changing to low glucose (**Supplementary Fig. 5b**,**c**).

To determine whether PKC-δ has a causal role in pericyte apoptosis and in the inhibition of PDGF-B actions, we transfected BRPCs with a control adenoviral vector expressing GFP (Ad-GFP) or with adenoviral vectors expressing either dominant-negative (Ad-DN) or wild-type (Ad-WT) PKC-δ isoforms. Pericytes transfected with Ad-GFP responded to high glucose similarly to untransfected cells, with a twofold increase in DNA fragmentation ($0.001 < P < 0.05$) (**Fig. 2e**). Transfection of Ad-WT PKC-δ but not Ad-WT PKC-β_2 increased DNA fragmentation by 30% and 50% ($P < 0.05$) in low-glucose and

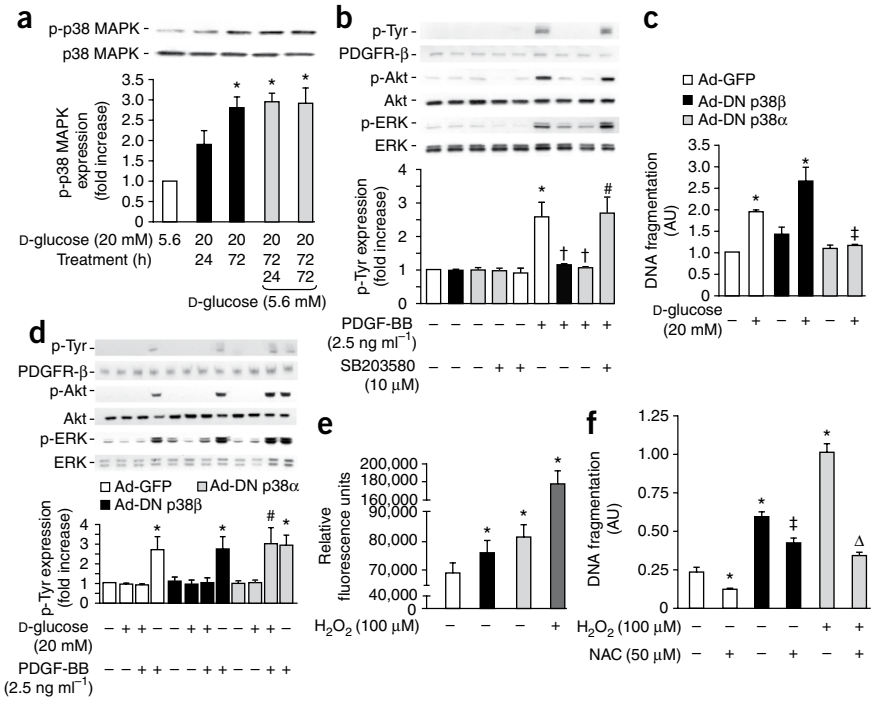

Figure 3 p38α MAPK is a downstream target by which hyperglycemia causes PDGF-B resistance and pericyte apoptosis. (**a**) Immunoblot analyses of phospho-p38 MAPK and p38 MAPK in BRPCs exposed to the indicated glucose conditions. (**b**) Immunoblot analyses of phospho-Tyr, PDGFR-β, phospho-Akt, Akt and phospho-ERK analysis (top) and densitometric quantification (bottom). Cells were exposed to LG (white bars), HG (black bars) or HG + LG (gray bars) in the presence or absence of SB203580; cells were then treated as indicated with PDGF-BB for 10 min. (**c**) DNA fragmentation in BRPCs exposed to LG (–) or HG (+) for 72 h and transfected with the indicated adenoviral constructs. (**d**) Immunoblot analyses of phospho-Tyr, PDGFR-β, phospho-Akt, Akt and phospho-ERK (top) and densitometric quantification (bottom). After transfection with the indicated adenoviral constructs and exposure to LG (–) or HG (+) for 72 h, cells were stimulated as indicated with PDGF-BB for 10 min. (**e**) ROS production, as measured in BPRCs exposed to LG (white bar), HG (black bar) or HG + LG (gray bar) and with H_2O_2 in LG as indicated, as described in the Online Methods section. (**f**) DNA fragmentation in BPRCs exposed to LG (white bars) or HG (black bars) for 72 h or H_2O_2 in LG (gray bars) for 2 h in the absence or presence of NAC. Results are shown as means ± s.d. of three to five independent experiments. *$P < 0.05$ versus LG, †$P < 0.05$ versus PDGF-BB in LG, ‡$P < 0.05$ versus HG in control or Ad-GFP-transfected cells in HG, #$P < 0.05$ versus HG + PDGF-BB in control or Ad-GFP–transfected cells, Δ$P < 0.05$ versus H_2O_2 in LG.

high-glucose conditions, respectively, whereas transfection of Ad-DN PKC-δ prevented the effects of high glucose on DNA fragmentation (**Fig. 2e** and **Supplementary Fig. 5d**). Moreover, brain pericytes isolated from diabetic *Prkcd*$^{+/+}$ mice, but not from diabetic *Prkcd*$^{-/-}$ mice, showed increased DNA fragmentation as compared to brain pericytes isolated from nondiabetic *Prkcd*$^{+/+}$ mice (**Supplementary Fig. 5e**). In low glucose conditions, PDGF-BB activated ERK and Akt phosphorylation in BRPCs by three- and fourfold ($P < 0.001$), respectively (**Fig. 2f**). These effects of PDGF-BB were impaired by 79–100% and by 67–100% in Ad-GFP– and Ad-WT PKC-δ–transfected pericytes when exposed to high-glucose as compared to low-glucose conditions, respectively, effects that were completely reversed in cells transfected with Ad-DN PKC-δ (**Fig. 2f**).

p38α MAPK is a target for high glucose effects

Because p38 MAPK expression induced by PKC-δ activation can cause cellular apoptosis[5,15], we explored whether p38 MAPK is involved in high glucose-dependent inhibition of PDGF signaling. High glucose induced p38 MAPK phosphorylation in BRPCs by 2.8-fold ($P < 0.001$), and this was not reversed by an additional 72-h exposure to low glucose (**Fig. 3a**). Inhibition of p38 MAPK using the compound SB203580 prevented high glucose–induced pericyte apoptosis, prevented inhibition of DNA synthesis and Akt and ERK phosphorylation and restored the effects of PDGF-BB treatment (**Fig. 3b** and **Supplementary Fig. 6a**,**b**). The α and β isoforms of p38 MAPK are the isoforms ubiquitously expressed in cells[16]. Immunoprecipitation studies in BRPCs exposed to low glucose, high glucose and high glucose plus low glucose showed that expression of p38α, but not p38β, was increased by high glucose conditions (**Supplementary Fig. 6c**). Therefore, we explored the role of each p38 MAPK isoform using adenoviral vector containing a dominant-negative form of either the p38α (Ad-DN p38α) or p38β (Ad-DN p38β) isoform. Transfection of Ad-DN p38α MAPK completely prevented ($P < 0.01$) the action of high glucose on pericyte apoptosis (**Fig. 3c**) and reversed high glucose–induced inhibition of PDGF-BB–mediated induction of Akt and ERK phosphorylation (**Fig. 3d**). Of note, transfection of Ad-DN p38β MAPK exacerbated the effects of high glucose on pericyte apoptosis and had no effect on the inhibition of PDGF-BB signaling (**Fig. 3c**,**d**). Reactive oxygen species (ROS) can also be increased by hyperglycemia and cause cellular apoptosis[17]. BRPCs exposed to high-glucose conditions increased ROS production by 11% ($P < 0.05$), which was not reversed by switching the cells to low-glucose conditions (**Fig. 3e**). However, treatment with *N*-acetylcysteine (NAC) only partially prevented high glucose–induced pericyte apoptosis, by 47% ($P < 0.05$), whereas this treatment completely prevented H_2O_2-induced cellular apoptosis (**Fig. 3f**). These results suggest that another pathway aside from oxidants is involved in hyperglycemia-induced pericyte apoptosis.

SHP-1 mediates PKC-δ and p38α MAPK actions on PDGFR-β

In considering how activation of PKC-δ and p38α MAPK inhibit PDGF signaling, we decided to evaluate SHP-1, which can bind PDGFR-β and inhibit its activation[18]. In BRPCs, high glucose increased SHP-1 expression by 81% ($P < 0.01$), and this increase in SHP-1 expression persisted even after cells were shifted to low glucose-conditions (**Fig. 4a**). Other PTPs, such as SHP-2 and PTP-1B, or lipid phosphatases, such as PTEN, were not affected (**Fig. 4a**). Notably, retinal pericytes isolated from diabetic rats and cultured in either low-glucose or high-glucose conditions had significantly elevated levels of PKC-δ and p38 MAPK phosphorylation and of SHP-1 expression as compared to those isolated from nondiabetic rats (**Fig. 4b**). In parallel, PKC-δ and SHP-1 mRNA expression in retinal pericytes isolated from diabetic rats were increased by 73% and 78%, respectively, compared to those isolated from nondiabetic rats, whereas expression of these genes was not affected in retinal endothelial cells, and ET-1 mRNA expression was elevated in both cell types by diabetes (**Supplementary Fig. 7a**). We demonstrated the functional importance of PKC-δ and p38 MAPK activation on high glucose-induced SHP-1 expression by showing that SB203580 treatment or Ad-DN PKC-δ transfection completely

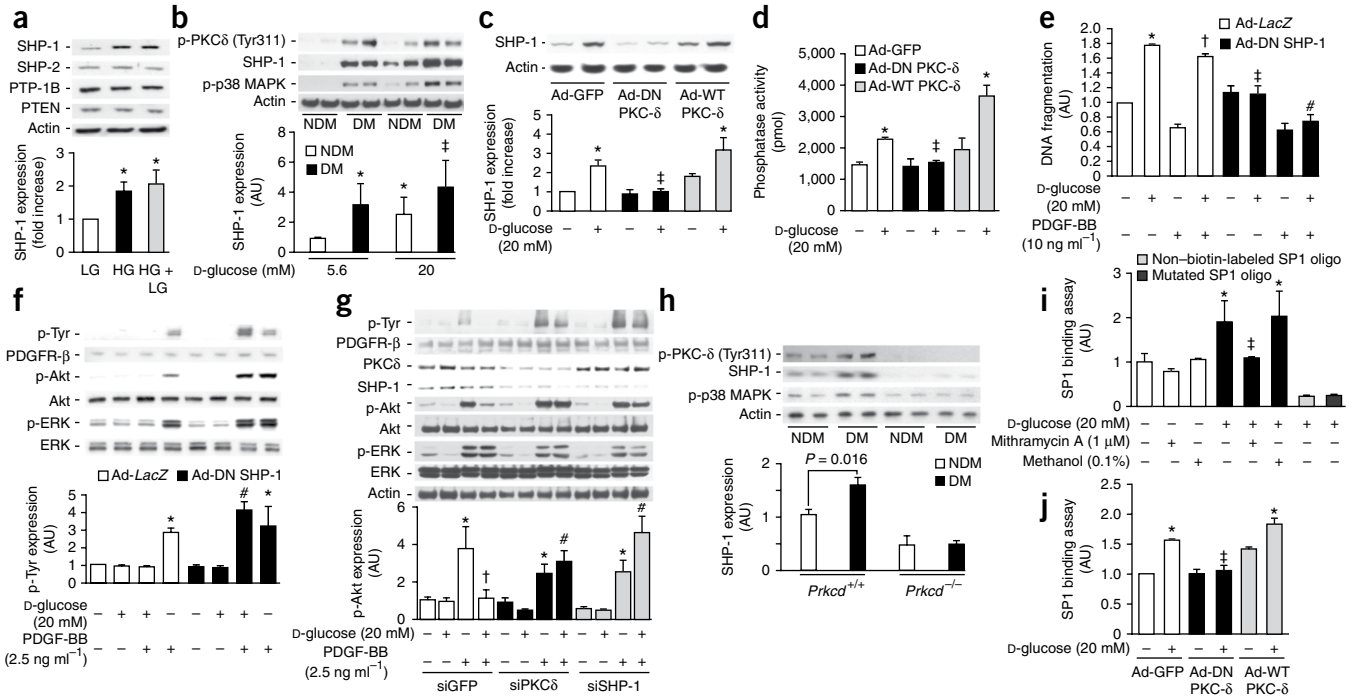

Figure 4 SHP-1 inhibits hyperglycemia– and PKC-δ and p38α MAPK–induced PDGF signaling pathway activation. (**a**) Immunoblot analyses of SHP-1, SHP-2, PTP-1B and phosphatase and tensin homolog (PTEN) normalized to actin expression in BRPCs exposed to LG, HG or HG + LG (top) and densitometric quantification of the blots (bottom). (**b**) Phospho–PKC-δ, p38 MAPK and SHP-1 protein expression in retinal pericytes isolated from NDM and DM rats ($n = 6$) cultured in LG or HG for 72 h. (**c**,**d**) SHP-1 expression levels (**c**) and phosphatase activity (**d**) in BRPCs transfected with the indicated adenoviral constructs and then incubated with LG (–) or HG (+) for 72 h. (**e**,**f**) Cells were transfected with the indicated adenoviral constructs and exposed to LG (–) or HG (+) for 72 h in the presence or absence of PDGF-BB. (**e**) Apoptosis, as measured by DNA fragmentation. (**f**) Immunoblot analyses of phospho-Tyr, phosphor–PKC-δ, PDGFR-β, phospho-Akt, Akt, phospho-ERK and ERK. (**g**) Immunoblot analyses of phospho-Tyr, phosphor–PKC-δ, PDGFR-β, phospho-Akt, Akt, phospho-ERK, ERK, PKC-δ and SHP-1 in BRPCs transfected with the indicated siRNA, exposed to LG (–) or HG (+) for 72 h and then stimulated with PDGF-BB. (**h**) Phospho-PKC-δ, p38 MAPK and SHP-1 protein expression in brain pericytes of NDM and DM *Prkcd*$^{+/+}$ and *Prkcd*$^{-/-}$ mice ($n = 4$) cultured in LG for 72 h. (**i**,**j**) Assay of SP1 transcriptional activity in BRPCs exposed to LG (–) or HG (+) in the presence or absence of mithramycin A or methanol (**i**) or BRPCs transfected with the indicated adenoviral constructs and then incubated with LG (–) or HG (+) for 72 h (**j**). (**b**,**c**,**f**,**g**,**h**) Immunoblot analyses of phospho-Tyr, phospho-PKC-δ, PDGFR-β, phospho-Akt, Akt, phospho-ERK, ERK, phospho-p38 MAPK, SHP-1 and actin (top) and densitometric quantification (bottom). Results are shown as means ± s.d. of three to five independent experiments. *$P < 0.05$ versus LG and LG in NDM, †$P < 0.05$ versus PDGF-BB in LG, ‡$P < 0.05$ versus HG or HG + LG or HG in Ad-GFP or Ad-*LacZ*–transfected cells or versus HG in siGFP–treated cells, #$P < 0.05$ versus HG + PDGF-BB in Ad-*LacZ*–transfected cells and in siGFP-treated cells.

prevented high glucose–induced SHP-1 protein expression ($P < 0.05$) (**Fig. 4c** and **Supplementary Fig. 7b**). Exposure of bovine retinal endothelial cells and BRPCs transfected with Ad-WT PKC-β to high glucose concentrations or the addition of H_2O_2 (100 μM) to BRPCs did not increase SHP-1 protein expression as compared to control conditions (**Supplementary Fig. 7c–e**). SHP-1 phosphatase activity increased in BRPCs by 57% ($P < 0.01$) with high glucose exposure and was not reversed by switching the cells to low-glucose conditions (**Supplementary Fig. 8a**); however, SHP-1 activity was reduced by 77% ($P < 0.01$) or 86% ($P < 0.05$) in cells treated with SB203580 (**Supplementary Fig. 8a**) or transfected with Ad-DN PKC-δ (**Fig. 4d**), respectively.

To study the functional role of SHP-1 in hyperglycemia, we used siRNA and an adenoviral vector containing dominant-negative SHP-1 (Ad-DN SHP-1). Transfection of Ad-DN SHP-1 or knockdown of SHP-1 or PKC-δ with siRNA in BRPCs not only completely inhibited high glucose–induced apoptosis but also restored the antiapoptotic and signaling actions of PDGF-BB as compared to GFP siRNA– or Ad-*LacZ*–transfected cells (**Fig. 4e–g** and **Supplementary Fig. 8b**). Our data also showed that high-glucose conditions increased the expression of cleaved caspase-8, and that transfection of either Ad-DN PKC-δ or Ad-DN SHP-1 prevented these effects (**Supplementary Fig. 8c**). These results may in part explain why inhibition of the PKC-δ–p38α MAPK–SHP-1 pathway in cultured cells can prevent pericyte apoptosis in high-glucose conditions alone. The levels of PKC-δ and p38 MAPK phosphorylation and of SHP-1 expression were also increased in brain pericytes isolated from diabetic *Prkcd*$^{+/+}$ but not *Prkcd*$^{-/-}$ mice compared those isolated from nondiabetic *Prkcd*$^{+/+}$ mice (**Fig. 4h**).

A specificity protein-1 (SP1) element is present in the promoter region of SHP-1 (ref. 19). We designed specific oligonucleotides to the SP1 sequence (GC box) located in the bovine SHP-1 promoter region to measure SP1 transcriptional binding activity. Exposure of BRPCs to high glucose increased SP1 binding activity in nuclear lysates, which could be suppressed by addition of either a SP1 inhibitor (mithramycin A), or non–biotin-labeled competitor oligonucleotides at a tenfold higher concentration than biotin-labeled DNA oligonucleotides of SP1; oligonucleotides with two mutations in the SP1 GC box sequence were used as a negative control (**Fig. 4i**). SP1 binding activity was also elevated in high glucose-treated cells transfected with Ad-GFP and Ad-WT PKC-δ but not in high glucose-treated cells transfected with Ad-DN PKC-δ (**Fig. 4j**). To confirm that hyperglycemia promotes SHP-1 expression by increasing the transcriptional activity of SP1, we treated BRPCs with mithramycin A, which prevented high glucose–induced SHP-1 expression as compared to vehicle (methanol)-treated or untreated cells (**Supplementary Fig. 8d**).

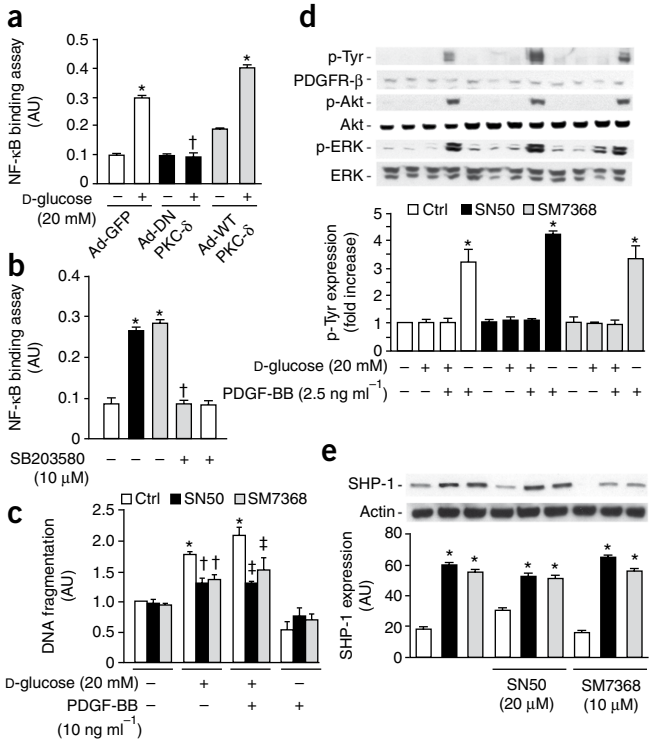

Figure 5 Hyperglycemia-induced increase of SHP-1 expression is independent of NF-κB activation. (**a**) Transcriptional binding activity assay of NF-κB in BRPCs transfected with the indicated adenoviral constructs and then incubated with LG (–) or HG (+) for 72 h. (**b**) Transcriptional binding activity assay of NF-κB in BRPCs treated with LG (white bars), HG (black bar) or HG + LG (gray bars) with or without SB203580. (**c**) DNA fragmentation in BRPCs incubated LG (–) or HG (+) in the absence (Ctrl) or presence of inhibitors of NF-κB (SN50 or SM7368). (**d**,**e**) Immunoblot analyses of phospho-Tyr, PDGFR-β, phospho-Akt, Akt, phospho-ERK and ERK (**d**) and SHP-1 (**e**) in BRPCs incubated as described in **c** and then stimulated with PDGF-BB for 10 min. In **e**, white bars, black bars and gray bars indicate LG, HG and HG + LG conditions, respectively. Densitometric quantification is shown below the blots. Results are shown as means ± s.d. of three to five independent experiments. $*P < 0.05$ versus LG, $\dagger P < 0.05$ versus Ad-GFP–transfected cells in HG or control cells in HG + LG, $\ddagger P < 0.05$ versus control cells in HG + PDGF-BB.

SHP-1 expression is independent of NF-κB activation

Activation of NF-κB has been reported to be involved in pericyte apoptosis induced by hyperglycemia[20]. Therefore, we evaluated the relationship between PKC-δ, p38α MAPK and SHP-1 activation, and NF-κB transcriptional activity. High glucose exposure of BRPCs increased the transcriptional activity of NF-κB in Ad-GFP– and Ad-WT PKC-δ–transfected cells by three- and fourfold ($P < 0.001$), respectively, but this effect was completely inhibited in Ad-DN PKC-δ–transfected pericytes (**Fig. 5a**). NAC treatment also completely prevented NF-κB transcriptional binding activity induced by either high-glucose conditions or H_2O_2 treatment (**Supplementary Fig. 9**). Furthermore, inhibition of p38 MAPK by SB203580 (10 μM) also prevented high glucose–induced NF-κB transcriptional activity ($P < 0.001$) (**Fig. 5b**). Selective inhibitors of NF-κB translocation to the nucleus (SN50) or DNA binding (SM7368) partially reduced high glucose–induced DNA fragmentation by 60% and 52% ($P < 0.01$), respectively (**Fig. 5c**). However, these compounds did not reverse the inhibitory actions of high glucose on PDGF's effects—either its antiapoptotic effects or its effects on the phosphorylation of ERK and Akt and on the phosphorylation of tyrosine residues of PDGFR-β (**Fig. 5c**,**d**). Inhibition of NF-κB with either SN50 or SM7368 also did not prevent the high glucose–induced increase in SHP-1 expression (**Fig. 5e**).

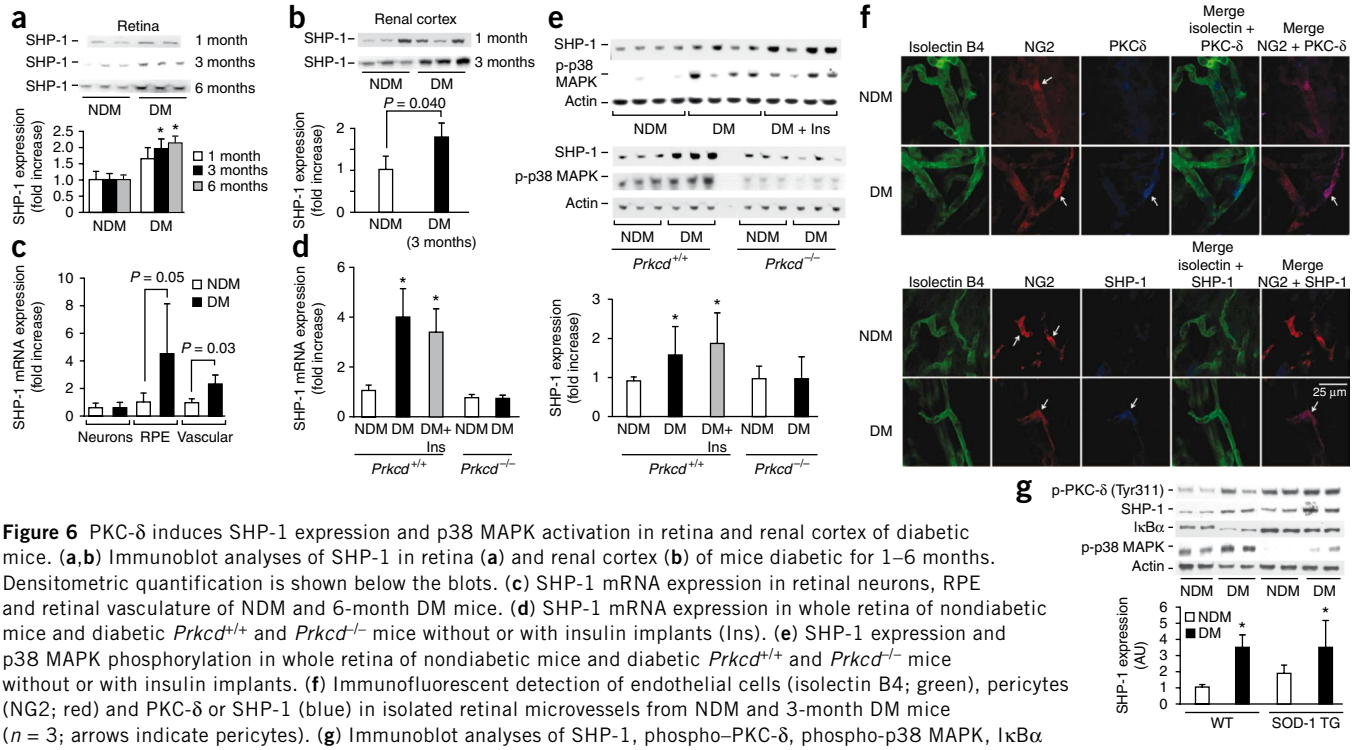

Figure 6 PKC-δ induces SHP-1 expression and p38 MAPK activation in retina and renal cortex of diabetic mice. (**a**,**b**) Immunoblot analyses of SHP-1 in retina (**a**) and renal cortex (**b**) of mice diabetic for 1–6 months. Densitometric quantification is shown below the blots. (**c**) SHP-1 mRNA expression in retinal neurons, RPE and retinal vasculature of NDM and 6-month DM mice. (**d**) SHP-1 mRNA expression in whole retina of nondiabetic mice and diabetic *Prkcd*$^{+/+}$ and *Prkcd*$^{-/-}$ mice without or with insulin implants (Ins). (**e**) SHP-1 expression and p38 MAPK phosphorylation in whole retina of nondiabetic mice and diabetic *Prkcd*$^{+/+}$ and *Prkcd*$^{-/-}$ mice without or with insulin implants. (**f**) Immunofluorescent detection of endothelial cells (isolectin B4; green), pericytes (NG2; red) and PKC-δ or SHP-1 (blue) in isolated retinal microvessels from NDM and 3-month DM mice ($n = 3$; arrows indicate pericytes). (**g**) Immunoblot analyses of SHP-1, phospho–PKC-δ, phospho-p38 MAPK, IκBα and actin in whole retinas of NDM and DM control nontransgenic and SOD-1–transgenic (TG) mice (top) and densitometric quantification (bottom). Results are shown as means ± s.d. of three to five independent experiments. $*P < 0.05$ versus NDM *Prkcd*$^{+/+}$ mice.

SHP-1 and p38α MAPK inhibition in diabetic *Prkcd*$^{-/-}$ pericytes

We assessed SHP-1 expression in several relevant tissues including the retina and renal cortex in diabetic mice. Expression of SHP-1 protein increased in the retina by 1.8- to twofold ($P < 0.05$) after 3 or 6 months of diabetes and in the renal cortex by 1.8-fold ($P < 0.05$) after 3 months of diabetes (**Fig. 6a**,**b**). Using laser capture microcopy, we found that the diabetic state increased SHP-1 mRNA expression in the retinal pigment epithelium (RPE) by fourfold ($P = 0.05$) and in vascular tissues by 2.1-fold ($P = 0.03$), but not in the retinal neuronal layers (**Fig. 6c**). We also evaluated the role of PKC-δ and the reversibility of SHP-1 mRNA expression in the retina. Expression of SHP-1 mRNA increased in the retina of diabetic *Prkcd*$^{+/+}$ mice after 6 months of diabetes (fourfold; $P < 0.001$) and remained elevated even after achieving euglycemia in the second 3-month period; however, SHP-1 mRNA expression was not different in diabetic *Prkcd*$^{-/-}$ mice as compared to nondiabetic controls (**Fig. 6d**). SHP-1 and phospho-p38 MAPK protein expression were elevated by 51% and 50% ($P < 0.01$), respectively, in the retinas of diabetic *Prkcd*$^{+/+}$ mice without and with treatment with insulin implants as compared to nondiabetic *Prkcd*$^{+/+}$ mice (**Fig. 6e**). In contrast, diabetic *Prkcd*$^{-/-}$ mice showed no changes in SHP-1 or phospho-p38 MAPK protein expression as compared to nondiabetic *Prkcd*$^{-/-}$ mice (**Fig. 6e**). By immunostaining for NG2, a marker for pericytes, we found that pericytes in the retinal microvessels of diabetic mice had higher levels of PKC-δ and SHP-1 expression as compared to microvessel pericytes from nondiabetic mice (**Fig. 6f**). In contrast, we did not find any apparent differences in the expression of PKC-δ or SHP-1 in retinal endothelial cells (as determined by staining for isolectin B4) between diabetic and nondiabetic mice (**Fig. 6f**).

Diabetes has been associated with elevated amounts of oxidative stress markers and with increased degradation of IκBα, an inhibitor of NF-κB signaling[21]. Although cytosolic superoxide dismutase (SOD-1)-transgenic diabetic mice had reduced oxidative stress plasma marker abundance (data not shown) and unelevated expression of IκBα protein in the retina compared to nontransgenic control diabetic mice, they had increased SHP-1 expression by 87% ($P < 0.05$) as compared to nondiabetic transgenic mice, a similar finding as in nontransgenic mice (**Fig. 6g**). These results suggest that elevated SHP-1 protein expression by hyperglycemia is not regulated by oxidative stress.

DISCUSSION

We have identified a series of common biochemical steps that are induced by hyperglycemia to activate NF-κB and PDGF-B resistance pathways to cause pericyte apoptosis, the most specific vascular histopathology associated with diabetic complications. These results show that hyperglycemia activates PKC-δ in a persistent manner, probably via an increase in transcription of the gene encoding PKC-δ. Hyperglycemia has previously been reported to increase PKC-β abundance in endothelial cells[22], but the consequences of activation of these two PKC isoforms are very different: PKC-δ activation is associated with cellular apoptosis, whereas PKC-β activation is known to enhance cellular growth[12,23]. Accordingly, we found that a sustained increase in PKC-δ levels for several months of diabetes correlated with the appearance of retinal pericyte apoptosis and acellular capillaries. In contrast, activation of PKC-β isoform in endothelial cells mediates an increase in ET-1 expression and enhances VEGF activity to cause endothelial dysfunction and to decrease RBF[24,25]. Clinical trials showed that a PKC-β–selective inhibitor delays the loss of visual acuity and progression of diabetic macular edema but does not affect the progression of proliferative diabetic retinopathy[26], suggesting that more than PKC-β activation is involved in the vascular pathology of diabetic retinopathy.

We found that hyperglycemia activates PKC-δ (but not PKC-β) specifically in pericytes, as shown using immunohistochemistry of retinal microvessels and pericytes isolated from diabetic rats. PKC-δ activation is required for pericyte apoptosis and other vascular pathology: diabetic *Prkcd*$^{-/-}$ mice are protected from pericyte loss, the formation of acellular capillaries and increased retinal permeability. A potential technical limitation of our work is that analyses of acellular capillaries and pericyte ghosts are performed after trypsin digestion and are morphological measures that imply the absence of pericytes, but these analyses cannot be definitively interpreted for identifying the cell type that died or the mechanism of cell death.

Our *in vivo* studies showed that PKC-δ activation leads to PDGF resistance in the retinas of diabetic mice; such resistance was not observed in *Prkcd*$^{-/-}$ mice. Moreover, specific inhibition of PKC-δ in pericytes *in vitro* or disruption of *Prkcd* in mice *in vivo* prevented SHP-1 expression and NF-κB activation, indicating that PKC-δ acts upstream of pathways mediated by both of these proteins. These findings identify a pivotal role for PKC-δ activation in causing pericyte apoptosis and the formation of acellular capillaries.

Multiple stimuli have been reported to increase the rate of PKC-δ gene transcription or to activate PKC-δ protein, including oxidative stress, ultraviolet light and other stresses[27]. Here, activation of PKC-δ and its elevated protein abundance persist in pericytes cultured from diabetic mice and rats, even after normoglycemia has been reinstituted. Our data suggest that chronic activation of PKC-δ is probably caused by effects on gene transcription rather than protein activation, as increased diacylglycerol concentrations are not maintained after switching high-glucose conditions to low-glucose conditions. However, it is possible that local and transient production of diacylglycerol may be sufficient to maintain PKC activity. In addition, high glucose seems to increase the rate of PKC-δ transcription, as expression of PKC-δ protein increases without parallel changes in the half-life of PKC-δ mRNA. Although the mechanisms underlying the persistent elevation of PKC-δ protein levels in pericytes are currently unclear, this finding is reminiscent of the persistent activation of NF-κB induced by hyperglycemia observed in monocytes, endothelial and smooth muscle cells, which has been attributed to epigenetic modification of histone methylation[28–30].

Our results suggest that a specific target of PKC-δ signaling leading to cellular apoptosis is p38α MAPK, whereas the p38β isoform does not seem to be involved. Several mechanisms could explain the activation of p38α MAPK by PKC-δ, including direct and, possibly, indirect activation of MAPK[13]. Our results are consistent with previous studies that have shown that p38α MAPK activation can be used as a proapoptotic marker, whereas p38β MAPK has been mainly associated with cell migration, transcriptional regulation of Bcl-2 and antiapoptotic effects[31,32].

Our results show that high glucose–induced activation of PKC-δ and p38α MAPK can cause pericyte apoptosis through two different pathways: a pathway involving ROS induction of NF-κB activity, and a pathway involving deactivation of PDGFR-β. High glucose–induced activation of p38α MAPK via NF-κB and the caspase pathway, causing apoptosis, has previously been reported[20]. This previous study and the results of our experiments using SOD-1–transgenic mice support the notion that oxidative stress induces the NF-κB pathway, which can cause pericyte apoptosis. However, we found

that treatment with two inhibitors of NF-κB and antioxidant only partially inhibit high glucose–induced pericyte apoptosis and do not prevent high glucose–induced inhibition of PDGF-BB's actions on Akt and ERK activation. In contrast, inhibition of PKC-δ and p38α MAPK was able to prevent completely high glucose– or diabetes-induced pericyte apoptosis. These results suggest that high glucose can induce pericyte apoptosis by acting downstream of p38α MAPK activation, partially via the known NF-κB cascade, and partially via an independent pathway that induces apoptosis through inhibition of the actions of PDGF.

Our findings identify SHP-1 as a previously unrecognized downstream target of PKC-δ and p38α MAPK. SHP-1 has been reported to downregulate several receptor tyrosine kinases, including PDGFR-β, the insulin receptor, the EGF receptor and VEGFR-2[17,33–35]. Mice deficient in SHP-1 due to mutation have severe hematopoietic disruption leading to patch dermatitis, extramedullary hematopoiesis, splenomegaly and hemorrhagic pneumonitis resulting in death after several weeks[36,37]. Therefore, we were not able to evaluate the consequences of SHP-1 deficiency in mice after 6 months of diabetes. SHP-1 may have direct effects on the retina, given that SHP-1–deficient mice show retinal photoreceptor dysfunction[38]. Notably, we found that dominant-negative SHP-1 or siRNA specific for SHP-1 in pericytes completely prevented high glucose–induced inhibition of PDGF signaling and induction of apoptosis. To our knowledge, we identify SHP-1 for the first time as a cellular target of p38α MAPK, which increases activity of the SP1 transcription factor and thereby increases SHP-1 expression. Increased levels of SHP-1, in turn, lead to induction of apoptosis via deactivation of the prosurvival action of growth factor receptors such as PDGFR-β, an NF-κB–independent pathway. Changes in SHP-1 expression in diabetic mice and rats, measured using cultured pericytes derived from these animals or using uncultured pericytes captured by retinal laser microdissection, indicated that changes in SHP-1 expression are sustained and are cell-type selective. Changes in SHP-1 expression are also found in other cell types and tissues in diabetic animals, such as RPE and perivascular cells (glial cells) in the retina and in renal podocytes, suggesting a more widespread involvement of SHP-1 in diabetic pathology. Based on our results, high glucose–induced PKC-δ and SHP-1 activation could cause cellular apoptosis, a common cellular feature of diabetic vascular complications involving the retina, renal glands and cardiovascular tissue.

In summary, we show that hyperglycemia activates two independently acting pathways—the first involving PKC-δ and p38α MAPK–mediated activation of SHP-1, resulting in PDGFR-β deactivation, and the second NF-κB-activation—to cause pericyte apoptosis in cultured cells and to initiate diabetic retinopathy *in vivo*. These findings identify several potential new therapeutic targets for the treatment of retinopathy and potentially other vascular complications of diabetes.

METHODS

Methods and any associated references are available in the online version of the paper at http://www.nature.com/naturemedicine/.

Note: Supplementary information is available on the Nature Medicine website.

ACKNOWLEDGMENTS

Prkcd$^{-/-}$ mice were provided by M. Leitges (University of Oslo). Adenoviral vectors expressing dominant-negative p38α and p38β MAPK were generously provided by Y. Wang (University of California, Los Angeles). Adenoviral vector expressing dominant-negative of SHP-1 (Ad-DN SHP-1) was generously provided by A. Marette (University of Laval). P.G. is a recipient of awards from the Juvenile Diabetes Research Foundation. This study was supported by the US National Eye Institute (grant 5R01EY016150-02to G.L.K.) and by the Canadian Institute of Health Research (grant 165453) to A.M. We thank W.-C. Li and S. Bonner-Weir for the technical support on confocal microscopy imaging.

AUTHOR CONTRIBUTIONS

P.G. and G.L.K. conceived of, designed and performed most of the research, analyzed the data and wrote the manuscript. J.H.-Y. and M.M. conducted the research experiments using the laser microdissection and rat studies. A.C. performed the RBF and MCT studies. M.L. provided the *Prkcd*$^{-/-}$ mice. A.M. provided the adenoviral vector encoding the dominant-negative form of SHP-1. L.P.A. conceived of and edited the manuscript. T.S.K. performed the acellular capillary and pericyte loss measurements, analyzed the data and edited the manuscript.

Published at http://www.nature.com/naturemedicine/.
Reprints and permissions information is available at http://npg.nature.com/reprintsandpermissions/.

1. Lorenzi, M. & Gerhardinger, C. Early cellular and molecular changes induced by diabetes in the retina. *Diabetologia* **44**, 791–804 (2001).
2. Isermann, B. *et al.* Activated protein C protects against diabetic nephropathy by inhibiting endothelial and podocyte apoptosis. *Nat. Med.* **13**, 1349–1358 (2007).
3. The Diabetes Control and Complications Trial Research Group. The effect of intensive treatment of diabetes on the development and progression of long-term complications in insulin-dependent diabetes mellitus. *N. Engl. J. Med.* **329**, 977–986 (1993).
4. Mizutani, M., Kern, T.S. & Lorenzi, M. Accelerated death of retinal microvascular cells in human and experimental diabetic retinopathy. *J. Clin. Invest.* **97**, 2883–2890 (1996).
5. Busik, J.V., Mohr, S. & Grant, M.B. Hyperglycemia-induced reactive oxygen species toxicity to endothelial cells is dependent on paracrine mediators. *Diabetes* **57**, 1952–1965 (2008).
6. Hammes, H.P. Pericytes and the pathogenesis of diabetic retinopathy. *Horm. Metab. Res.* **37** Suppl 1, 39–43 (2005).
7. Writing Team for the Diabetes Control and Complications Trial/Epidemiology of Diabetes Interventions and Complications Research Group. Sustained effect of intensive treatment of type 1 diabetes mellitus on development and progression of diabetic nephropathy: the Epidemiology of Diabetes Interventions and Complications (EDIC) study. *J. Am. Med. Assoc.* **290**, 2159–2167 (2003).
8. Kuwabara, T. & Cogan, D.G. Retinal vascular patterns. VI. Mural cells of the retinal capillaries. *Arch. Ophthalmol.* **69**, 492–502 (1963).
9. Frank, R.N. Diabetic retinopathy. *N. Engl. J. Med.* **350**, 48–58 (2004).
10. Enge, M. *et al.* Endothelium-specific platelet-derived growth factor-B ablation mimics diabetic retinopathy. *EMBO J.* **21**, 4307–4316 (2002).
11. Yokota, T. *et al.* Role of protein kinase C on the expression of platelet-derived growth factor and endothelin-1 in the retina of diabetic rats and cultured retinal capillary pericytes. *Diabetes* **52**, 838–845 (2003).
12. Koya, D. & King, G.L. Protein kinase C activation and the development of diabetic complications. *Diabetes* **47**, 859–866 (1998).
13. Ryer, E.J. *et al.* Protein kinase C δ induces apoptosis of vascular smooth muscle cells through induction of the tumor suppressor p53 by both p38-dependent and p38-independent mechanisms. *J. Biol. Chem.* **280**, 35310–35317 (2005).
14. Park, J.Y. *et al.* Induction of endothelin-1 expression by glucose: an effect of protein kinase C activation. *Diabetes* **49**, 1239–1248 (2000).
15. Igarashi, M. *et al.* Glucose or diabetes activates p38 mitogen-activated protein kinase via different pathways. *J. Clin. Invest.* **103**, 185–195 (1999).
16. Zarubin, T. & Han, J. Activation and signaling of the p38 MAP kinase pathway. *Cell Res.* **15**, 11–18 (2005).
17. Brownlee, M. Biochemistry and molecular cell biology of diabetic complications. *Nature* **414**, 813–820 (2001).
18. Yu, Z. *et al.* SHP-1 associates with both platelet-derived growth factor receptor and the p85 subunit of phosphatidylinositol 3-kinase. *J. Biol. Chem.* **273**, 3687–3694 (1998).
19. Nakase, K., Cheng, J., Zhu, Q. & Marasco, W.A. Mechanisms of SHP-1 P2 promoter regulation in hematopoietic cells and its silencing in HTLV-1-transformed T cells. *J. Leukoc. Biol.* **85**, 165–174 (2009).
20. Romeo, G., Liu, W.H., Asnaghi, V., Kern, T.S. & Lorenzi, M. Activation of nuclear factor-κB induced by diabetes and high glucose regulates a proapoptotic program in retinal pericytes. *Diabetes* **51**, 2241–2248 (2002).
21. Shoelson, S.E., Lee, J. & Goldfine, A.B. Inflammation and insulin resistance. *J. Clin. Invest.* **116**, 1793–1801 (2006).
22. Suzuma, K. *et al.* Characterization of protein kinase C beta isoform's action on retinoblastoma protein phosphorylation, vascular endothelial growth factor-induced endothelial cell proliferation, and retinal neovascularization. *Proc. Natl. Acad. Sci. USA* **99**, 721–726 (2002).

23. Idris, I., Gray, S. & Donnelly, R. Protein kinase C activation: isozyme-specific effects on metabolism and cardiovascular complications in diabetes. *Diabetologia* **44**, 659–673 (2001).
24. Ishii, H. *et al.* Amelioration of vascular dysfunctions in diabetic rats by an oral PKC beta inhibitor. *Science* **272**, 728–731 (1996).
25. Aiello, L.P. *et al.* Vascular endothelial growth factor in ocular fluid of patients with diabetic retinopathy and other retinal disorders. *N. Engl. J. Med.* **331**, 1480–1487 (1994).
26. The PKC-diabetic retinopathyS Study Group. The effect of ruboxistaurin on visual loss in patients with moderately severe to very severe nonproliferative diabetic retinopathy: initial results of the Protein Kinase C β Inhibitor Diabetic Retinopathy Study (PKC-diabetic retinopathyS) multicenter randomized clinical trial. *Diabetes* **54**, 2188–2197 (2005).
27. Kanthasamy, A.G., Kitazawa, M., Kanthasamy, A. & Anantharam, V. Role of proteolytic activation of protein kinase Cδ in oxidative stress–induced apoptosis. *Antioxid. Redox Signal.* **5**, 609–620 (2003).
28. Miao, F. *et al.* Genome-wide analysis of histone lysine methylation variations caused by diabetic conditions in human monocytes. *J. Biol. Chem.* **282**, 13854–13863 (2007).
29. El-Osta, A. *et al.* Transient high glucose causes persistent epigenetic changes and altered gene expression during subsequent normoglycemia. *J. Exp. Med.* **205**, 2409–2417 (2008).
30. Villeneuve, L.M. *et al.* Epigenetic histone H3 lysine 9 methylation in metabolic memory and inflammatory phenotype of vascular smooth muscle cells in diabetes. *Proc. Natl. Acad. Sci. USA* **105**, 9047–9052 (2008).
31. Peter, P.S. *et al.* Inhibition of p38 α MAPK rescues cardiomyopathy induced by overexpressed β2-adrenergic receptor, but not β1-adrenergic receptor. *J. Clin. Invest.* **117**, 1335–1343 (2007).
32. Nemoto, S., Xiang, J., Huang, S. & Lin, A. Induction of apoptosis by SB202190 through inhibition of p38β mitogen-activated protein kinase. *J. Biol. Chem.* **273**, 16415–16420 (1998).
33. Dubois, M.J. *et al.* The SHP-1 protein tyrosine phosphatase negatively modulates glucose homeostasis. *Nat. Med.* **12**, 549–556 (2006).
34. Tenev, T. *et al.* Both SH2 domains are involved in interaction of SHP-1 with the epidermal growth factor receptor but cannot confer receptor-directed activity to SHP-1/SHP-2 chimera. *J. Biol. Chem.* **272**, 5966–5973 (1997).
35. Bhattacharya, R., Kwon, J., Wang, E., Mukherjee, P. & Mukhopadhyay, D. Src homology 2 (SH2) domain containing protein tyrosine phosphatase-1 (SHP-1) dephosphorylates VEGF receptor-2 and attenuates endothelial DNA synthesis, but not migration*. *J. Mol. Signal.* **3**, 8 (2008).
36. Shultz, L.D. *et al.* Mutations at the murine motheaten locus are within the hematopoietic cell protein-tyrosine phosphatase (*Hcph*) gene. *Cell* **73**, 1445–1454 (1993).
37. Bignon, J.S. & Siminovitch, K.A. Identification of PTP1C mutation as the genetic defect in motheaten and viable motheaten mice: a step toward defining the roles of protein tyrosine phosphatases in the regulation of hemopoietic cell differentiation and function. *Clin. Immunol. Immunopathol.* **73**, 168–179 (1994).
38. Lyons, B.L. *et al.* Deficiency of SHP-1 protein-tyrosine phosphatase in "viable motheaten" mice results in retinal degeneration. *Invest. Ophthalmol. Vis. Sci.* **47**, 1201–1209 (2006).

ONLINE METHODS

Animals and experimental design. *Prkcd*$^{-/-}$ mice were produced as described previously and provided by M. Leitges[39]. *Prkcd*$^{-/-}$ and age-matched control *Prkcd*$^{+/+}$ mice with a mixed background of 129SV and C57BL/6J were crossbred for eight generations with wild-type C57BL/6J mice obtained from The Jackson Laboratory. We purchased SOD-1–transgenic mice and nontransgenic C57BL/6J mice (used as controls) from The Jackson Laboratory. We used *Prkcd*$^{-/-}$ mice, SOD-1–transgenic mice and age-matched control mice at 7–8 weeks of age. We rendered mice and rats diabetic by streptozotocin (Sigma) (90 mg per kg body weight in 0.05 M citrate buffer, pH. 4.5, intraperitoneally) on two consecutive days after overnight fasting; we injected control mice with citrate buffer. After 3 months of diabetes, we gave mice insulin implants (Linbit, LinShin Canada) subcutaneously to normalize their blood glucose level. We obtained male Sprague-Dawley rats from Charles River Laboratories. All experiments followed the guidelines of the Association for Research in Vision and Ophthalmology and were approved by the Animal Care and Use Committees of the Joslin Diabetes Center, according to US National Institutes of Health guidelines.

Blood glucose and insulin concentrations. We measured blood glucose by Glucometer (Elite, Bayer Inc). We measured plasma insulin concentrations with a rat insulin ELISA kit (Crystal Chem Inc.) according to the manufacturer's instructions.

Quantification of pericyte loss. We isolated the retinal vasculature by a trypsin digest method as previously described[40] and air-dried the vasculature onto glass slides. We then stained sections of the vasculature with hematoxylin and periodic acid–Schiff, dehydrated them and added coverslips[40]. We estimated the number of protruding 'bumps' in the capillary basement membranes lacking a pericyte, calling them pericyte ghosts. We quantified acellular capillaries in at least 1,000 capillary cells in four to seven field areas (400× magnification) in the mid-retina in a blinded manner. We identified acellular capillaries as capillary-sized vessel tubes having no nuclei anywhere along their length including or not vessel 'clusters', and we reported them per square millimeter of retinal area. To count acellular capillaries, we examined at least 1,000 capillary cells (endothelial cells and pericytes) in five field areas in the mid-retina (400× magnification) in a blinded manner. We quantified pericyte loss as the combined number of pericyte ghosts and acellular capillaries.

Cell culture. We obtained fresh calf eyes from a local slaughterhouse. We isolated primary cultures of mouse brain pericytes, rat retinal pericytes, rat retinal endothelial cells, bovine retinal pericytes and bovine retinal endothelial cells by homogenization and a series of filtration steps as described previously[41]. We subsequently propagated bovine retinal pericytes and rat endothelial cells in DMEM and 10% FBS, 100 μg ml^{-1} heparin and 50 μg ml^{-1} endothelial cell growth factor (Roche Applied Science) and grown them on collagen I–coated dishes (BD Biosciences). We cultured BRPCs, mouse brain pericytes and rat retinal pericytes in DMEM and 20% FBS. We characterized the purity of the pericyte cultures by immunoreactivity with monoclonal antibody 3G5 (ref. 42). We used cells from passages 2 through 5. We exposed cells to 5.6 mM glucose (low glucose) or 20 mM glucose (high glucose) for 72 h or 6 days; in some cases cells exposed to high glucose for 72 h were returned to low glucose for 72 h (high glucose plus low glucose) or in H_2O_2 for 2 h. Low serum conditions (1% FBS) were used. We adjusted the osmotic pressure in low glucose conditions by adding 14.6 mM mannitol.

Measurement of diacylglycerol concentrations. We measured total diacylglycerol levels with a radioenzymatic assay kit (Amersham) using diacylglycerol kinase, which quantitatively converts diacylglycerol to [^{32}P]phosphatidic acid in the presence of [γ-^{32}P]-ATP (New England Nuclear). We normalized diacylglycerol levels by the amount of cellular protein.

Immunohistochemistry. We isolated retinal microvessels from nondiabetic and diabetic mice and fixed them with 4% paraformaldehyde for 1 h on a cover slip. We blocked tissues with 10% goat serum for 1 h, exposed them in sequence to isolectin B4-FITC and primary antibodies (NG2, PKC-δ or SHP-1, 1 in 100) overnight followed by incubation with secondary antibodies (dylight-649–conjugated antibody specific for mouse IgG (115-496-146, 1 in 500) or 7-amino-4-methylcoumarin-3-acetic acid–conjugated antibody specific for rabbit IgG (111-155-003, 1 in 500, Jackson ImmunoResearch Laboratories). We captured confocal images on a Zeiss LSM 410 microscope; for each experiment, we obtained all images in the same sitting using identical settings and we handled all images similarly in Adobe Photoshop.

Phosphatase assay. We assessed phosphatase activity of SHP-1 using the RediPlate 96 EnzChek Tyrosine Phosphatase Assay kit (Invitrogen) according to the manufacturer's instructions. We immunoprecipitated SHP-1 from cell and tissue lysates with a polyclonal antibody (Santa Cruz Laboratories, clone C19) prebound to protein A Sepharose beads. After overnight incubation, we washed beads three times with PBS containing 1% Igepal CA-630 and 5 mM dithiothreitol. We placed beads into RediPlate wells and incubated them for 30 min at 20–22 °C before taking fluorescence readings.

Adenoviral vector transfection. We constructed adenoviral vectors containing green fluorescent protein (GFP, Ad-GFP), *LacZ* (Ad-*LacZ*) and dominant-negative or wild-type PKC-δ isoforms (Ad-DN PKC-δ and Ad-WT PKC-δ) and used them to infect pericytes as we have reported previously for various types of vascular and pancreatic cells[22,43]. Adenoviral vectors used to express dominant-negative p38α and p38β MAPK isoforms were generously provided by Y. Wang[44]. Adenoviral vector of dominant-negative of SHP-1 (Ad-DN SHP-1) was generously provided by A. Marette[33].

Statistical analyses. The data are shown as means ± s.d. for each group. We performed statistical analyses by unpaired *t* test or by one-way analysis of variance followed by Tukey's test correction for multiple comparisons. All results were considered statistically significant at $P < 0.05$.

Additional methodology. Measurement of PKC activity; laser capture microdissection; intracellular ROS production; assay of SP1 transcription factor activity; immunoblot analyses; real-time PCR analysis; adenoviral vector transfection; DNA fragmentation analysis to measure apoptosis; DNA synthesis analysis to measure cell proliferation; measurements of MCT, RBF, retinal permeability and vascular permeability; and reagents and antibodies are described in the **Supplementary Methods**.

39. Leitges, M. *et al.* Exacerbated vein graft arteriosclerosis in protein kinase Cδ-null mice. *J. Clin. Invest.* **108**, 1505–1512 (2001).
40. Kern, T.S. & Engerman, R.L. Comparison of retinal lesions in alloxan-diabetic rats and galactose-fed rats. *Curr. Eye Res.* **13**, 863–867 (1994).
41. King, G.L., Berman, A.B., Bonner-Weir, S. & Carson, M.P. Regulation of vascular permeability in cell culture. *Diabetes* **36**, 1460–1467 (1987).
42. Lindahl, P., Johansson, B.R., Leveen, P. & Betsholtz, C. Pericyte loss and microaneurysm formation in PDGF-B–deficient mice. *Science* **277**, 242–245 (1997).
43. Kanwar, M., Chan, P.S., Kern, T.S. & Kowluru, R.A. Oxidative damage in the retinal mitochondria of diabetic mice: possible protection by superoxide dismutase. *Invest. Ophthalmol. Vis. Sci.* **48**, 3805–3811 (2007).
44. Wang, Y. *et al.* Cardiac muscle cell hypertrophy and apoptosis induced by distinct members of the p38 mitogen-activated protein kinase family. *J. Biol. Chem.* **273**, 2161–2168 (1998).